Decolourization of malachite green dye by mentha plant biochar (MPB): a combined action of adsorption and electrochemical reduction processes

Abhay Prakash Rawat and D. P. Singh

ABSTRACT

Adsorption behavior of mentha (mint) plant biochar (MPB) in removal of malachite green (MG) dye from aqueous solution was analyzed as a function of different pH (4.0–10.0), initial dye concentration (20–100 mg/L), contact time (0–45 min) and dose of adsorbent (0.05–0.3 g/100 mL). The zeta potential of the MPB particles was found to be −37.9 mV, indicating a negatively charged sorption surface of MPB particles. MPB was found to be more effective in removal of MG dye at pH 6.0 due to combined action of physico-chemisorption and a reductive electron transfer reaction. Results on the Brunauer–Emmett–Teller (BET) analysis of the N_2 adsorption–desorption isotherm of MPB as adsorbent showed sigmoidal shape similar to the type IV isotherm and mesoporous nature. The cyclic voltammetric analysis of MG dye showed a reversible, coupled redox reaction at the interface of dye molecules and MPB particles. The maximum monolayer adsorption capacity (q_{max}) of MPB was found to be 322.58 mg g^{-1}. The separation factor (R_L) value was between 0 and 1, indicating a favourable adsorption of MG dye onto MPB. The results fitted well to a pseudo-second-order kinetic model. Further results from desorption experiments showed recovery of MG dye by about 50% in the presence of 1 N HCl.

Key words | adsorption, decolourization, electrochemical reduction, kinetics, malachite green, mentha plant biochar

Abhay Prakash Rawat
D. P. Singh (corresponding author)
Department of Environmental Science,
Babasaheb Bhimrao Ambedkar University,
Lucknow, Uttar Pradesh 226025,
India
E-mail: *dpsinghbbau@gmail.com*

INTRODUCTION

Food industries, printing, textiles, dyeing and dye stuff manufacturing are the main sources of dye-containing wastewater discharges into natural water bodies (Mittal *et al.* 2010). Large-scale production and application of organic dyes can potentially cause serious environmental and human health problems, as many dyes used in industrial processes are quite stable against photobleaching and are also resistant to aerobic digestion because of their structural complexity and large molecular size (Dincer *et al.* 2007). In addition, many dyes are highly visible in water at low concentrations (less than 1 mg/L for some dyes), which is enough to present an aesthetic problem (Low *et al.* 2012; Subramonian & Wu 2014). Malachite green (MG) dye has been widely used for dyeing leather, wool, jute and silk due to its low cost, easy availability, efficacy and lack of a proper alternative (Zhang *et al.* 2008). MG dye has properties that make it mutagenic and carcinogenic in nature and it is acutely toxic to a wide range of aquatic life. Several physico-chemical and biological methods have been employed to remove the dyes from wastewater (Lee *et al.* 2007). Activated carbon has good adsorption capacity but it is considered an expensive adsorbent. This has led many workers to search for cheap and efficient alternative adsorbents. A number of non-conventional and low cost agrowastes like palm ash, bottom ash, fly ash, bagasse fly ash and rice husk, etc., have been tried (Gupta *et al.* 2003; Janos *et al.* 2003; Malik & Saha 2003; Ahmad *et al.* 2007; Dincer *et al.* 2007).

Since India is the major producer of mentha (mint) oil in the world followed by China and Brazil, it produces mentha crop waste to the tune of approximately 1.8 to 2.0 tonnes $acre^{-1}$ yr^{-1} (Singh *et al.* 2010a, 2010b). Dried mentha plant waste is often used as fuel for steam distillation of mentha oil or else the mentha plant residues are left in the field with no subsequent application. Solid residue of *Mentha piperita* is available in plenty as a byproduct of the mentha distilling industry.

doi: 10.2166/wst.2018.059

Therefore, the main objective of the present study was to use the mentha plant waste after oil distillation for preparation of biochar and evaluate the sorption efficiency of mentha plant biochar (MPB) as an efficient adsorbent for removal of cationic dye (MG) from aqueous solutions. Physico-chemical studies of the adsorbent (MPB) were carried out to understand the characteristics of MPB. Effects of different environmental conditions such as pH, adsorbent dose, initial dye concentrations and contact time were evaluated to define the optimum conditions for the sorption process.

MATERIALS AND METHODS

Biochar preparation and characterization

The oil extracted mentha plant waste was collected from the oil distillation unit and was washed with distilled water to remove adhering dirt. The plant waste was oven dried at 60–80 °C for 4 h to remove moisture from plant stems. The resultant plant stems after removing leaves were crushed or cut to small pieces (30–50 mm) for the preparation of biochar. Further, the chopped material was placed in a 100 mL silica crucible (Product No. 842 – 100A, Swastic Scientific Co., India) covered with a lid and heated in a muffle furnace (Bio Technics BTI-36 1130 °C 2000 watt) at 400 °C for 2 h. The resultant carbon (biochar) was cooled in a desiccator and homogenized to a fine powder with a pestle and mortar. Finally the powder was sieved (<0.21 mm) by using 70-mesh size sieve and sieved powder was placed in air tight glass bottles so that it could be used for future study without any pre-treatment.

A zeta potential analyzer (Malvern Instruments Ltd, Serial Number: MAL1010294) was used to measure the surface potential of MPB particles. The sample of MPB was prepared by dissolving 1.0 mg of biochar in 10 mL of distilled water and was sonicated before analysis. The zeta potential spectrum was recorded in the range of −200 to 200 mV.

Specific surface area and other textural characteristics of MPB were determined using a Brunauer–Emmett–Teller (BET) instrument (BEL Master™ Ver.2.3.1, BEL Japan, Inc.). The Barrett–Joyner–Hanlenda (BJH) method was used to measure pore-size distributions of MPB particles.

X-ray diffraction (XRD) analysis of the MPB sample was carried out using a PANalytical XRD instrument (Model/Supplier: Panalytical), operated at 30 mA and 40 kV. The XRD data were collected over in the range of $2\theta = 5$–50° by step scanning using Cu Kα ($\lambda = 0.154$ nm) radiation.

Cyclic voltammetry (BASi EC Epsilon) instrument was used to determine electrochemical behaviour of MG dye in aqueous solution. The cyclic voltammetric (CV) test was performed in a single compartment with 50 mL of MG dye solution (50 mg L^{-1}) at pH 6.0 treated with MPB for 30 min at room temperature. The redox behaviour of MG dye was studied over a potential range from −1.5 V to +1.5 V (vs. Ag/AgCl) with a scan rate of 100 mVs^{-1} and step potential of 0.002 V.

The Fourier transform infrared spectroscopy (FTIR) spectrum (400–4,000 cm^{-1}) was determined before and after adsorption of MG onto MPB using a Thermo Scientific, USA; Model: Nicolet™ 6700 FTIR instrument.

Adsorption experiments

Batch experiments were carried out to examine the adsorption potential of MPB for the removal of MG in an orbital shaking incubator (Model UTS: 1.21) at 180 rpm, using conical flasks of 250 mL. The sorption of MG dye by MPB was carried out as a function of different contact time (0–45 min), adsorbent dose (0.05–0.3 g/100 mL), pH condition (4–10) and initial dye concentration (20–100 mg L^{-1}). To study the effect of contact time, pH and dye concentration on the sorption of MG, an amount of 0.1 g of MPB was added to 250 mL conical flasks containing 100 mL of 50 mg L^{-1} dye solution (pH 6.0) and the resulting solutions were placed under shaking condition (180 rpm) at an incubation temperature of 32 °C (approximately room temperature) for various time durations ranging from 5 min to 45 min. To study the effect of pH, the dye solution was prepared using appropriate buffer (20 mM) and shaken at 32 °C for 45 min.

All the working solutions were centrifuged (Remi Instruments Ltd: AXCI-7182) at 5,000 rpm for 10 min to separate dye-loaded adsorbent from the suspension. The final dye concentration in the supernatant was evaluated by measuring the concentration of dye at 618 nm wavelength using a UV–visible double beam spectrophotometer (Shimadzu UV–1601). The amount of dye adsorbed at equilibrium, q_e (mg g^{-1}) was calculated by the following equations:

$$q_e = \frac{(C_i - C_e)\mathrm{V}}{\mathrm{m}} \quad (1)$$

where C_i, C_e, V and m stand for initial dye concentration (mg L^{-1}), final dye concentration in solution (mg L^{-1}),

volume (L) of the solution and mass (g) of the adsorbent, respectively.

Adsorption isotherms

Langmuir isotherms were plotted to determine maximum adsorption capacity of adsorbent and constants were derived using the following equation:

$$\frac{C_e}{q_e} = \frac{1}{q_{max}\mathrm{b}} + \frac{C_e}{q_{max}} \quad (2)$$

where q_e, q_{max} and b are equilibrium adsorption capacity (mg g^{-1}), Langmuir constant related to the maximum adsorption capacity and adsorption energy, respectively.

The Freundlich isotherm was applicable to adsorption on heterogenous surfaces and constants were derived by using the following equation:

$$\mathrm{Log}\, q_e = \log K_F + 1/n \log Ce \quad (3)$$

where K_F is the adsorption capacity (mg g^{-1}) and n is the intensity of adsorption.

Sorption kinetics

Kinetic models (pseudo-first-order, pseudo-second-order and intraparticle diffusion) were applied to experimental data to find the best fit model for the sorption process. In kinetic studies, the amount of dye uptake q_t (mg g^{-1}) at time t, was calculated by the following equation:

$$q_t = \frac{(C_0 - C_t)\mathrm{V}}{\mathrm{m}} \quad (4)$$

where C_0 and C_t are the dye concentration in solution (mg L^{-1}) before and after time t.

The pseudo- first-order kinetics can be described by the following equation:

$$\log (q_e - q_t) = \frac{\log q_e - k_1 \mathrm{t}}{2.303} \quad (5)$$

where k_1 (min^{-1}) is first-order rate constant and q_e (mg g^{-1}) is the equilibrium adsorption capacity.

The pseudo-second-order kinetic model can be expressed in linear form as:

$$\frac{\mathrm{t}}{\mathrm{qt}} = \frac{1}{k_2 q_e^2} + \frac{\mathrm{t}}{q_e\, \mathrm{t}} \quad (6)$$

where k_2 (g mg^{-1} min^{-1}) is second-order rate constant.

The intra-particle diffusion model as applied in sorption process of MG by MPB is described by the following equation:

$$q_t = k_{id} t^{1/2} + C \quad (7)$$

where C and k_{id} (mg/g $min^{1/2}$) are the constants related to intercept and diffusion rate constant, respectively.

Desorption of dye

In the desorption study, 100 mL of MG dye solution (50 mg L^{-1}) was mixed with adsorbent MPB (0.1 g/100 mL) at pH 6.0 and the resulting solutions was placed under shaking (180 rpm) at 32 °C for 45 min. The dye-loaded MPB was separated by centrifugation and the residual MG dye concentration in the supernatant was measured to determine the amount of dye adsorbed by MPB particles. Thereafter, 0.1 g of dye-loaded dried MPB (dried at 70 °C for 6–8 h) was added to 100 mL of desorbing solution (1.0 N each of HCl, CH_3COOH, H_2SO_4 and NaOH) and the mixture was shaken at 180 rpm for 45 min. The amount of dye released in the desorbing solution was determined by using UV-visible double beam spectrophotometer (Shimadzu UV-1601) as described earlier. The adsorbent (MPB) separated from the desorbing solution was washed with the distilled water 3 to 4 times to remove the desorbing solution from the MPB. The washed MPB particles were dried at 70 °C for 6–8 h for further use. In the present study, use of 1N desorbing solution of acids or alkali to desorb the MG dye was preferred so that the surface characteristics of biochar (MPB) were not severely modified. The percent desorption of dye was calculated at regular time intervals by the following equation:

$$\text{Percent desorption}(\%) = \frac{\text{Amount of dye desorbed}}{\text{Amount of dye adsorbed}} \times 100 \quad (8)$$

RESULTS AND DISCUSSION

Characterization of adsorbent (MPB)

In order to see the role of surface charge on adsorption, the zeta potential of MPB was calculated to be −37.9 mV. This result indicates that the surface of MPB particles have a moderate negative charge. The zeta potential curve measured on MPB is shown in Figure 1(a). The

electronegative surface of MPB might be due to the presence of minerals and unburnt biomolecules in the biochar. It is desirable that an electronegative surface of MPB can be more helpful for adsorption of cationic dye like MG (Bootharaju & Pradeep 2013).

The BET analysis of the N_2 adsorption–desorption isotherm provides valuable information about surface area and porosity of the material (Mall *et al.* 2006). The N_2 adsorption–desorption isotherm measured on MPB at 77 K has been shown in Figure 1(b). The shape of the isotherm matches the Type IV shape of adsorption isotherm (IUPAC classification), indicating a mesoporous structure of MPB. The characteristics of Type IV isotherm correspond with monolayer-multilayer adsorption and are indicative of relatively strong interaction between adsorbent surface and adsorbate as suggested by earlier workers (Sing *et al.* 1985). In the present study, the BET specific surface area, total pore volume and average pore diameter were found to be 1.058 $m^2 g^{-1}$, 0.0035 $cm^{-3} g^{-1}$ and 12.91 nm, respectively. The pore size distribution of MPB particles, as determined by BJH model, were found to be in the range of 3–20 nm, indicating the mesoporous nature of material. A pore diameter in adsorbent particles between 2 to 50 nm indicates a mesoporous material (Sing *et al.* 1985).

The XRD pattern of MPB is shown in Figure 1(c). The presence of calcite, quartz, ankerite, sylvite and lithiophorite were confirmed by their inter-atomic distance (*d*) in the random powder diffraction pattern of the MPB. Quartz (SiO_2) and calcite ($CaCO_3$) are the two most common crystalline phases identified in the biochars derived from different biomass wastes. Calcite is one of the main constituents of ash and biochar derived from several plant and tree species (Singh *et al.* 2010a, 2010b). The peak at 3.033 Å (*d* value given in Å) was attributed to the presence of calcite ($CaCO_3$), whereas the occurrence of quartz (SiO_2) was identified by peaks at 4.257 and 3.341 Å. The presence of ankerite, sylvite and lithiophorite were detected by peaks at 2.191, 3.151 and 9.280 Å, respectively. Higher XRD peak intensities at 3.341 Å and 3.033 Å, indicated a well crystalline form of quartz and calcite, respectively, when compared with the peak intensities of ankerite, sylvite and lithiophorite (Singh *et al.* 2010a, 2010b).

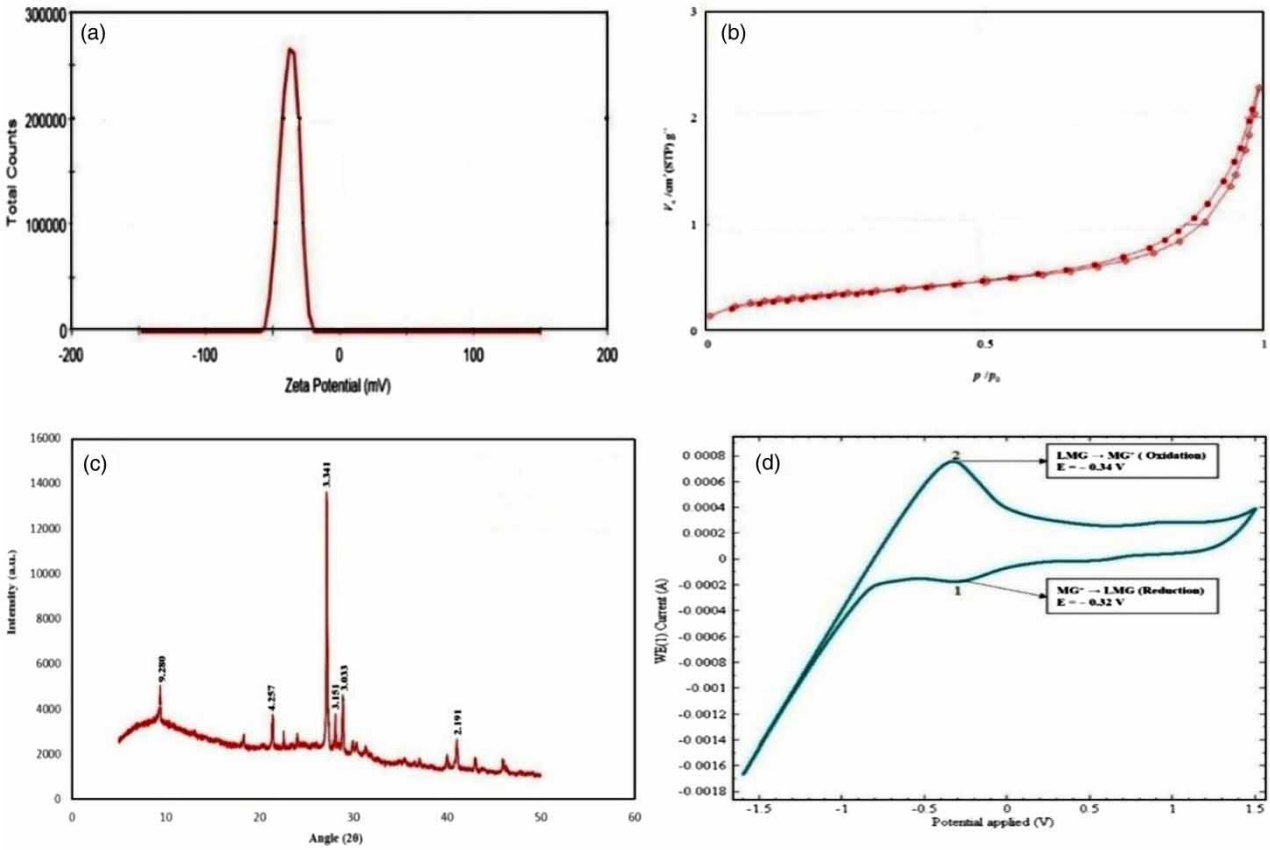

Figure 1 | Physico-chemical characterization of MPB (a) zeta potential curve, (b) nitrogen adsorption–desorption isotherm, (c) XRD pattern (Peaks indicated by *d* values given in Å) and (d) cyclic voltammogram of MG dye.

CV analysis was performed on the MG dye solution obtained after treatment with MPB. The cyclic voltammogram of MG dye (Figure 1(d)) in the electrolytic solution showed a well-defined redox couple. Results of the CV test showed cathodic and anodic activities of MG dye in aqueous solution, indicating reduction of MG dye by biochar particles involves electron transfer process (Ngamukot *et al.* 2006). In the cyclic voltammogram of MG dye, the peak 1 (cathodic) appearing at approximately −0.32 V was assigned to the reduction of MG^+ to neutral leuco malachite green (LMG) by one electron transfer reaction (Ngamukot *et al.* 2006), where peak 2 (anodic) at −0.34 V might be related to oxidation of neutral LMG to MG^+. The coupled redox reaction for MG dye in the CV test suggested that MG^+ cations adsorbed on the surface of biochar particles were changed to LMG through a reversible electron transfer reaction. The several minerals and surface active ligands in MPB might be contributing as electron donors for adsorbent mediated reduction of MG dye.

The FTIR spectra (Figure 2) of the adsorbent (MPB) before and after dye adsorption was obtained to study the surface characteristics of adsorbent. The recorded IR spectrum of a dye-loaded MPB sample showed changes in the IR adsorption characteristics of different functional groups which might be involved in the process of MG dye adsorption. The changes in IR absorption peaks appearing at 3,827.7 cm^{-1} and 3,748.5 cm^{-1}, assigned to phenolic groups, indicated the role played by these functional groups in dye binding on the MPB surface (Ahmad *et al.* 2007). The IR peaks at wavenumber 3,038.3 cm^{-1}, assigned to alkanes, completely disappeared after the treatment of MPB with MG dye. A new IR peak at wavenumber 2,904.4 cm^{-1} (Mohan 2005) suggested new bonding between the ligands and dye molecules. The IR peaks at wavenumber of 2,878.8 and 2,828.7 cm^{-1} assigned to aliphatic and aldehyde groups, respectively, completely disappeared after adsorption of MG dye onto MPB (Mohan 2005), again indicated strong interaction between organic moieties and dye molecules. The peak at wavenumber 1,580.0 cm^{-1} assigned to carboxyl anions and stretching of the C = O group in proteins, and emergence of a new peak at wavenumber 1,433.0 cm^{-1} (Sun *et al.* 2013), indicated involvement of hydroxyl and acetal functional groups in the dye binding. An intense band occurring at wavenumber 1,032.5 cm^{-1} indicated C–O stretching in phenolic or alcoholic groups. The observed changes in IR peaks after MG dye binding indicated that several functional groups on the surface of the MPB adsorbent played important roles in interaction with dye, indicative of chemisorption process.

Effect of adsorbent dose

The adsorption capacity is greatly influenced by the dose of MPB (adsorbent) in removal of MG dye from aqueous solution. The amount of dye adsorbed by MPB was studied

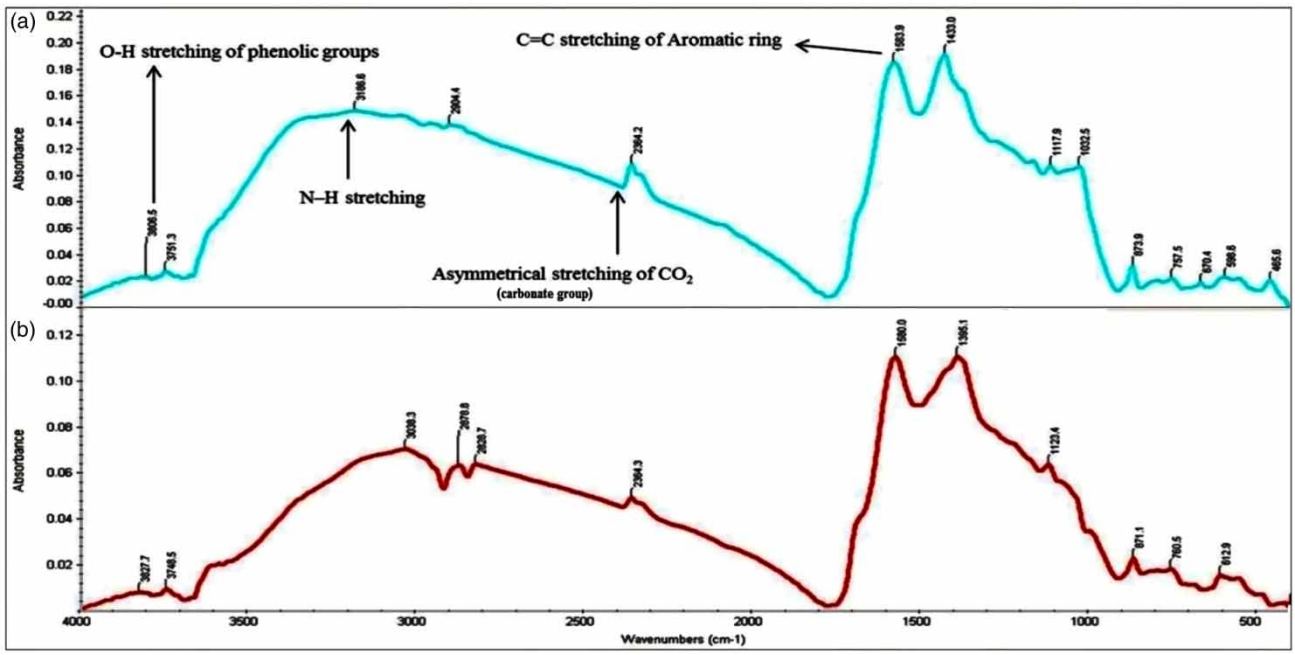

Figure 2 | FTIR (Mid) stack image of MPB (a) after and (b) before adsorption of MG dye.

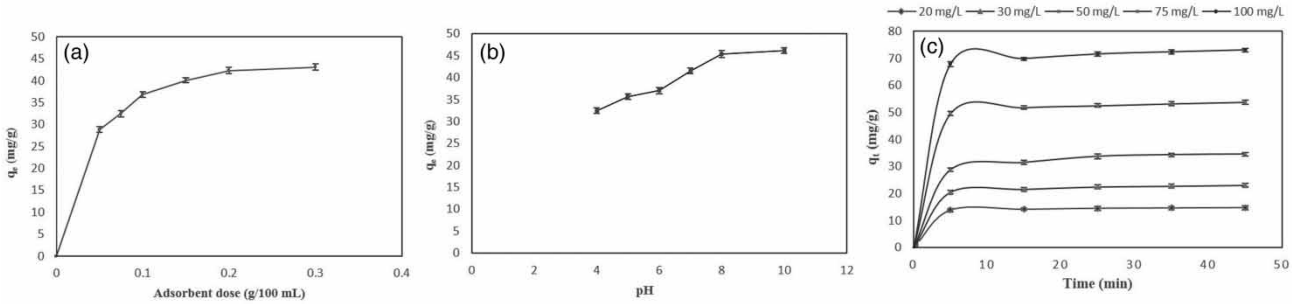

Figure 3 | Effect of (a) adsorbent dose, (b) pH and (c) initial dye concentration on the sorption of MG dye by MPB. (Error bars indicate the standard deviation with in a single sample measured three times.)

as a function of adsorbent doses (0.05 to 0.3 g/100 mL) at 50 mg L^{-1} dye concentration for 45 min. As shown in Figure 3(a), the dye uptake increased from 28.81 to 43.11 mg g^{-1} with increase in adsorbent dose from 0.05 to 0.3 g/100 mL. A rapid phase of dose-dependent increase in dye removal occurred up to 0.1 g/100 mL dose of MPB and this was followed by a sluggish phase of dye removal between 0.1 to 0.3 g/100 mL of dose of adsorbent. The maximum dye removal, at an adsorbent dose of 0.1 g/100 mL, was found to be 36.86 mg g^{-1}. As the number of available adsorption sites increased in a dose-dependent manner, the rate of dye removal also increased. A sluggish increase in dye binding at higher doses of adsorbent (0.1 to 0.3 g/100 mL) may be due to less availability of dye molecules per unit concentration of adsorbent. Otherwise, it may be stated that the clustering of adsorbent particles per unit volume might be hindering the free mobility of the dye molecules approaching to the binding sites on the surface of adsorbent (Garg *et al.* 2003).

Effect of pH

The pH of the dye solution can influence the surface potential of the adsorbent, as well as chemistry of adsorbate (Shayesteh *et al.* 2015). In the present study, the effect of pH (pH 4–10) on the sorption of MG dye by MPB was studied, at fixed concentration of dye (50 mg L^{-1}) and adsorbent (0.1 g/100 mL). As shown in Figure 3(b), the amount of dye adsorbed at equilibrium (q_e) increased from 32.41 to 46.21 mg g^{-1} with increase in the pH from 4.0 to 10.0. The results showed least adsorption of MG dye at acidic pH 4.0 perhaps due to reduction in the electronegative moieties on the adsorbent surface (MPB). Besides, protonation of the MG dye molecules at acidic pH might be inhibiting the active binding between the adsorbent and dye. A high rate of dye removal at pH 10.0 could be due to increase in the negatively charged moieties on the surface of the adsorbent, which facilitate the binding of cationic MG dye. Earlier, workers have also demonstrated a high rate of MG dye removal at pH 10.0 by spent tea active carbon (Akar *et al.* 2013). Earlier findings have also demonstrated that an increase in electrostatic interaction between the dye molecule and surface binding ligands is responsible for an initial fast rate of dye adsorption (Mittal *et al.* 2010).

Effect of initial dye concentration and contact time

The effect of initial dye concentration on the adsorption capacity of MPB depends on the availability of dye molecules and surface binding sites of MPB particles. The extent of dye removal is greatly influenced by initial dye concentration in aqueous solution. In the present study, the effect of different initial concentration of MG dye (20 to 100 mg $L^{-1)}$ was studied on the adsorption of MG dye for 45 min at a fixed dose of adsorbent (0.1 g/100 mL) at room temperature and pH 6.0. The results in Figure 3(c), on the adsorption of MG dye by MPB showed initially a very rapid process upto 5 min, followed by slowing down of the process with increase in the contact time up to 45 min, perhaps due to non-availability of adsorption sites on the surface of adsorbent (Saha *et al.* 2010). Further removal of dye after 45 min was found to be insignificant. A rapid rate of dye adsorption at the initial contact time could be attributed to the availability of a large number of adsorption sites. The rate of dye binding increased in a concentration-dependent manner and the saturation concentration of dye at equilibrium (q_e) was found to increase from 14.73 to 73.03 mg g^{-1} with an increase in the initial dye concentration from 20 to 100 mg L^{-1}. An increase in adsorption capacity of MPB with increase in MG dye concentrations, might be due to relatively higher rate of mass transfer (Bulut & Aydin 2006). But the sluggish increase in

Table 1 | Langmuir and Freundlich constants for the sorption of MG by MPB

Langmuir constants			Freundlich constants		
q_m (mg g^{-1})	b (L mg^{-1})	R^2	Adsorption intensity (n)	Adsorption coefficient K_F (mg/g)	R^2
322.58	0.00106	0.989	1.066	0.3269	0.981

the rate of dye adsorption at higher concentration could be attributed to a limiting dose of adsorbent (Garg *et al.* 2003).

Adsorption isotherms

The values of isotherm constants and their respective correlation coefficients R^2 are given in Table 1. The calculated R^2 values suggested that both the Langmuir and Freundlich isotherm models fitted well with the data on equilibrium adsorption of MG dye. The maximum monolayer sorption capacity (q_{max}), according to the Langmuir isotherm model, was found to be 322.58 mg g^{-1} at room temperature. A comparative list of q_{max} values (adsorption capacities) of different biosorbents is given in Table 2.

The values of the separation factor (R_L) were found to be in the range of 0.98–0.91 (Supplementary Table S1, available with the online version of this paper) at different concentrations of MG (20 to 100 mg g^{-1}), indicating favorable adsorption of MG dye onto MPB. A value of R_L between 0 and 1 always is indicative of favourable adsorption of adsorbate with greater affinity for adsorbent as suggested by Ma *et al.* (2015).

In the Freundlich model, the value of n (1.067) indicated favourable adsorption of MG dye onto MPB by physico-chemisorption on heterogenous surface of MPB. It has been suggested that the value of n between 1 and 10 represents a beneficial sorption process. The calculated value of K_F in the Freundlich isotherm was 0.327, suggesting efficient adsorption of MG dye by MPB.

Adsorption kinetics

The three different kinetic models previously presented were fitted to the experimental data for different initial concentrations of MG dye (20–100 mg L^{-1}) to examine the adsorption mechanisms involved in removal of MG dye by MPB. All the calculated kinetic parameters and the values of correlation coefficients (R^2) are given in Table 3. It can be simply confirmed that the pseudo-first-order kinetics is not applicable for MG dye binding with biochar as the calculated q_e values from pseudo-first-order kinetic model were not in good agreement with the experimental q_e values. The value of $R^2 > 0.99$ for the pseudo-second-order kinetics was higher than R^2 value (>0.97) for the pseudo-first-order kinetics. Thus, the results suggested that pseudo-second-order kinetic model fitted well with adsorption kinetics of MG dye, whereas pseudo-first-order kinetic model did not fit well with the experimental data for the sorption of MG dye onto MPB. These results further indicated that the rate of adsorption of MG dye onto MPB was almost a controlled chemisorption process, which involved sharing of electrons between the surface ligands of biochar and dye molecules. Similar observations were reported for sorption of basic dye onto activated carbon prepared from rattan saw dust (Hameed *et al.* 2007).

The plot of q_t versus $t^{1/2}$ showed linear regression and passes through the origin at each concentration of MG dye, indicating that intra-particle diffusion could be the rate controlling step. The rate constant (K_{id}) and intercept (C) are presented in Table 3. The intercept C of the linear

Table 2 | Adsorption capacities (mg g^{-1}) of different biosorbents for the sorption of MG dye

Adsorbents	q_{max} (mg g^{-1})	pH	Temp (K)	References
Degreased coffee bean	55.3	4.0	298	Baek *et al.* (2010)
Activated carbon (AC)	75.08	10.0	–	Gupta *et al.* (1997)
Banana stalk-AC	141.76	8.0	303	Bello *et al.* (2012)
Spent tea leaves-AC	256.40	4.0–11.0	318	Akar *et al.* (2013)
Chlorella biomass	18.4	7.0	298	Tsai & Chen (2010)
Borassus bark carbon	20.7	6.0	303	Arivoli *et al.* (2009)
Rambutan peel-AC	329.49	>8.0	303	Ahmad & Alrozi (2011)
MPB	322.58	6.0	303	This study

Table 3 | Kinetic parameters at different dye concentration in the sorption of MG dye by MPB

		First-order kinetics			Second-order kinetics				Intra-particle diffusion model		
Conc (mg/L)	Exp. q_e (mg/g)	k_1 (1/min)	Cal. q_e (mg/g)	R^2	k_2 (mg/g min)	Cal. q_e (mg/g)	R^2	Initial adsorption rate (h) H (mg g^{-1} min^{-1})	K_{id} (mg/g $min^{1/2}$)	C	R^2
20	14.73	0.064	1.35	0.973	0.208	14.75	0.999	45.05	0.21	13.36	0.979
30	22.99	0.069	3.78	0.991	0.078	23.1	0.999	41.35	0.58	19.25	0.979
50	34.49	0.113	12.59	0.975	0.035	34.97	0.999	42.57	1.36	26.09	0.945
75	53.83	0.063	5.63	0.986	0.051	53.77	0.999	147.1	0.91	47.88	0.973
100	73.03	0.069	7.94	0.989	0.038	73	0.999	200.04	1.19	65.3	0.991

plot reflects boundary layer diffusion. The larger the value of C, the greater the contribution of the surface sorption as the rate controlling step. When the linear plot at every concentration does not pass through the origin, this is the indicative of some degree of involvement of a boundary layer in controlling diffusion, not only intraparticle diffusion (Alzaydien 2009).

A high value of initial adsorption rate h (200.04 mg g^{-1} min^{-1}) for MPB at high dye concentration (100 mg L^{-1}) indicated that the sorption of MG onto MPB might be carried out through surface interchange reactions until the surface functional sites are occupied (Ma *et al.* 2015). The h value increased from 45.05 to 200.04 mg g^{-1} min^{-1} with increase in the initial concentration of MG dye (Table 3). The intra-particle diffusion model did not as well as the pseudo-second-order model.

Desorption of MG dye

The desorbing solutions of mineral acids (1N HCl and H_2SO_4) were found to be more effective in desorption of MG dye from dye loaded MPB adsorbent. The percent desorption of MG dye in different desorbing agents are presented in Supplementary Table S2 (available with the online version of this paper). A percentage de-sorption (49.55%) of MG dye by mineral acid (HCl) indicated that the dye was adsorbed onto MPB by a physico-chemical sorption process as suggested by earlier workers (Mall *et al.* 2006). The desorbing agent (HCl) reduced the pH of solution and, hence, at acidic pH, the surface of MPB becomes more protonated and the attachment between dye molecules and MPB is weakened due to electrostatic repulsion as MG is a positively charged dye. The lowest percentage of desorption (6.53%) was observed with 1N of NaOH as desorbing solution perhaps on account of strong affinity of the adsorbent for the cationic adsorbate at alkaline pH. Desorption process is always inversely proportional to bond strength of adsorbed material, a strong interaction between the dye and MPB could be the reason for weak desorption of MG dye.

CONCLUSIONS

MPB, derived from waste plant residues, is an efficient adsorbent for removal of MG dye. The process of MG dye adsorption is found to be dependent on initial dye concentration, dose of adsorbent, pH and contact time. The optimum pH for the adsorption of MG dye onto MPB was between pH 6–8 and the time to reach equilibrium was 15 min. FTIR analysis of MPB in the presence of MG dye showed changes in the IR peaks of MPB, indicating involvement of surface binding ligands (amine, phenyl, hydroxyl, carbonyl and carboxyl groups, etc.) in the dye binding. Results on kinetics, and adsorption isotherms indicated that the process of adsorption is an energetically favourable physico-chemisorption process. The cyclic voltammetry analysis indicated a reversible, redox coupled electrochemical reduction of dye mediated by MPB. Thus, the MPB mediated decolourization of MG dye at higher dye concentrations involves both physico-chemisorption, as well as electrochemical reduction of dye. Further, the added advantage associated with MPB is that the resource material is easily available in plenty as a byproduct of mentha oil distillation units.

ACKNOWLEDGEMENTS

The authors acknowledge the Head, Department of Environmental Science and Director, University Science

Instrumentation Centre (USIC), Babasaheb Bhimrao Ambedkar University, Lucknow for providing laboratory facility to perform the experiments. We are grateful to the UGC, New Delhi for providing RGNF to Mr Abhay P. Rawat.

REFERENCES

Ahmad, M. A. & Alrozi, R. 2011 Removal of malachite green dye from aqueous solution using rambutan peel-based activated carbon: equilibrium, kinetic and thermodynamic studies. *Chemical Engineering Journal* **171**, 510–516.

Ahmad, A. A., Hameed, B. H. & Aziz, N. 2007 Adsorption of direct dye on palm ash: kinetic and equilibrium modeling. *Journal of Hazardous Materials* **141**, 70–76.

Akar, E., Altinişik, A. & Seki, Y. 2013 Using of activated carbon produced from spent tea leaves for the removal of malachite green from aqueous solution. *Ecological Engineering* **52**, 19–27.

Alzaydien, A. S. 2009 Adsorption of methylene blue from aqueous solution onto a low cost natural Jordanian Tripoli. *American Journal of Environmental Sciences* **5**, 197–208.

Arivoli, S., Hema, M., Martin, P. & Prasath, D. 2009 Adsorption of malachite green onto carbon prepared from borassus bark. *Arabian Journal for Science and Engineering* **34**, 31–42.

Baek, M. H., Ijagbemi, C. O., Se-Jin, O. & Kim, D. S. 2010 Removal of malachite green from aqueous solution using degreased coffee bean. *Journal of Hazardous Materials* **176**, 820–828.

Bello, O. S., Ahmad, M. A. & Ahmad, N. 2012 Adsorptive features of banana (*Musa paradisiaca*) stalk-based activated carbon for malachite green dye removal. *Chemistry and Ecology* **28**, 153–167.

Bootharaju, M. S. & Pradeep, T. 2013 Facile and rapid synthesis of a dithiol-protected Ag7 quantum cluster for selective adsorption of cationic dyes. *Langmuir* **29**, 8125–8132.

Bulut, Y. & Aydın, H. 2006 A kinetics and thermodynamics study of methylene blue adsorption on wheat shells. *Desalination* **194**, 259–267.

Dincer, A. R., Gunes, Y., Karakaya, N. & Gunes, E. 2007 Comparison of activated carbon and bottom ash for removal of reactive dye from aqueous solution. *Bioresource Technology* **98**, 834–839.

Garg, V. K., Gupta, R., Yadav, A. B. & Kumar, R. 2003 Dye removal from aqueous solution by adsorption on treated sawdust. *Bioresource Technology* **89**, 121–124.

Gupta, V. K., Srivastava, S. K. & Mohan, D. 1997 Equilibrium uptake, sorption dynamics, process optimization, and column operations for the removal and recovery of malachite green from wastewater using activated carbon and activated slag. *Industrial and Engineering Chemistry Research* **36**, 2207–2218.

Gupta, V. K., Jain, C. K., Imran, A., Sharma, M. & Saini, V. K. 2003 Removal of cadmium and nickel from waste water using bagasse fly ash – a sugar industry waste. *Water Research* **37**, 4038–4044.

Hameed, B. H., Ahmad, A. L. & Latiff, K. N. A. 2007 Adsorption of basic dye (methylene blue) onto activated carbon prepared from rattan sawdust. *Dyes and Pigments* **75**, 143–149.

Janos, P., Buchtova, H. & Ryznarova, M. 2003 Sorption of dyes from aqueous solutions onto fly ash. *Water Research* **37**, 4938–4944.

Lee, C. K., Liu, S. S., Juang, L. C., Wang, C. C., Lin, K. S. & Lyu, M. D. 2007 Application of MCM-41 for dyes removal from wastewater. *Journal of Hazardous Materials* **147**, 997–1005.

Low, F. C. F., Wu, T. Y., Teh, C. Y., Juan, J. C. & Balasubramanian, N. 2012 Investigation into photocatalytic decolorisation of CI Reactive Black 5 using titanium dioxide nanopowder. *Coloration Technology* **128**, 44–50.

Ma, H., Li, J. B., Liu, W. W., Miao, M., Cheng, B. J. & Zhu, S. W. 2015 Novel synthesis of a versatile magnetic adsorbent derived from corncob for dye removal. *Bioresource Technology* **190**, 13–20.

Malik, P. K. & Saha, S. K. 2003 Oxidation of direct dyes with hydrogen peroxide using ferrous ion as catalyst. *Separation and Purification Technology* **31**, 241–250.

Mall, I. D., Srivastava, V. C. & Agarwal, N. K. 2006 Removal of orange-G and methyl violet dyes by adsorption onto bagasse fly ash – kinetic study and equilibrium isotherm analyses. *Dyes and Pigments* **69**, 210–223.

Mittal, A., Mittal, J., Malviya, A., Kaur, D. & Gupta, V. K. 2010 Adsorption of hazardous crystal violet from waste water by waste materials. *Journal of Colloid and Interface Science* **343**, 463–473.

Mohan, J. 2005 *Organic Spectroscopy Principles and Applications*, 2nd edn. Narosa Publishing House, New Delhi, India.

Ngamukot, P., Charoenraks, T., Chailapakul, O., Motomizu, S. & Chuanuwatanakul, S. 2006 Cost-effective flow cell for the determination of malachite green and leucomalachite green at a boron-doped diamond thin-film electrode. *Analytical Sciences* **22**, 111–116.

Saha, P., Chowdhury, S., Gupta, S. & Kumar, I. 2010 Insight into adsorption equilibrium, kinetics and thermodynamics of malachite green onto clayey soil of Indian origin. *Chemical Engineering Journal* **165**, 874–882.

Shayesteh, H., Kelishami, A. R. & Norouzbeigi, R. 2015 Adsorption of malachite green and crystal violet cationic dyes from aqueous solution using pumice stone as a low-cost adsorbent: kinetic, equilibrium and thermodynamic studies. *Desalination and Water Treatment* **57**, 12822–12831.

Sing, K. S. W., Everett, D. H., Haul, R. A. W., Moscou, L., Pierotti, R. A., Rouquerol, J. & Siemieniewska, T. 1985 Reporting physisorption data for gas/solid systems with special reference to the determination of surface area and porosity. *Pure and Applied Chemistry* **57**, 603–619.

Singh, B., Singh, B. P. & Cowie, A. L. 2010a Characterization and evaluation of biochars for their application as a soil amendment. *Australian Journal of Soil Research* **48**, 516–525.

Singh, S. M., Gangwar, G. R., Prakash, O. & Rachna 2010b Biocomposting of extracted peppermint plant residue

(*Menthapiperita*) using red worm, *Eiseniafetida* and its effect on the growth of *Vignamungo* (Urad). *Journal of Applied and Natural Science* **2**, 305–312.

Subramonian, W. & Wu, T. Y. 2014 Effect of enhancers and inhibitors on photocatalytic sunlight treatment of methylene blue. *Water, Air, and Soil Pollution* **225**, 1–15.

Sun, L., Wan, S. & Luo, W. 2013 Biochars prepared from anaerobic digestion residue, palm bark, and eucalyptus for adsorption of cationic methylene blue dye: characterization, equilibrium, and kinetic studies. *Bioresource Technology* **140**, 406–413.

Tsai, W. T. & Chen, H. R. 2010 Removal of malachite green from aqueous solution using low-cost *Chlorella* based biomass. *Journal of Hazardous Materials* **175**, 844–849.

Zhang, J., Li, Y., Zhang, C. & Jing, Y. 2008 Adsorption of malachite green from aqueous solution onto carbon prepared from Arundo donax root. *Journal of Hazardous Materials* **150**, 774–782.

First received 16 August 2017; accepted in revised form 29 January 2018. Available online 14 February 2018